Article ID: 1003－6326(2004)03－0436－05

Electrochemical hydrogen storage properties of $La_{0.95}Mg_{2.05}Ni_9$ alloy prepared by mechanical alloying①

MENG Miao-wu(蒙冕武)[1,3], LIU Xin-yu(刘心宇)[1,2], CHENG Jun(成 钧)[2], ZHOU Huai-ying(周怀营)[2]
(1. College of Materials Science and Engineering, Central South University, Changsha 410083, China;
2. Center of Materials Science and Engineering,
Guilin University of Electronic Technology, Guilin 541004, China;
3. Department of Resources and Environmental Science,
Guangxi Normal University, Guilin 541004, China)

Abstract: The structure, microstructure, thermal stability and hydriding characteristics of amorphous $La_{0.95}Mg_{2.05}Ni_9$ have been investigated with differential thermal analysis, X-ray diffraction, scanning electron microscopy and battery test. It is found that the increase in mechanical alloying time leads to enhancement in thermal stabilities of amorphous $La_{0.95}Mg_{2.05}Ni_9$ alloy. The amorphous alloy has good charge/discharge ability at room temperature(430 mA·h·g^{-1}), but the discharge capacity decreases seriously during cycling tests due to the crystallization of amorphous and oxidization of magnesium on the particle surface in alkaline aqueous solution.

Key words: mechanical alloying; hydrogen storage material; amorphous alloy; electrochemical properties; thermal stability

CLC number: TG 146.45 **Document code:** A

1 INTRODUCTION

The Mg-based hydrogen storage alloys as the active materials of metal hydride electrodes have attracted attention because of higher theoretical capacities for hydrogen absorption/desorption, and the lower price compared with the other hydrides[1-7]. Recently, the charge-discharge properties of Mg-based alloys at room temperature have been greatly improved by some researchers[8-13].

In particular, the Mg-Ni-RE system alloy is one of the most promising hydrides[14-16]. Tanaka et al[15] reported that the nanocrystalline Mg-Ni-RE (RE= La, Nd) alloys prepared by melt-spinning and crystallization exhibit excellent hydrogen absorbing kinetics and PCT characteristics in comparison with those of the corresponding as-cast alloys with coarse eutectic structure. Kohno et al[16] also reported that the La_2MgNi_9, $La_5Mg_2Ni_{23}$, La_3MgNi_{14} ternary system alloys are composed of stacked AB_5 and AB_2 structure subunits in a superstructure arrangement, and the $La_5Mg_2Ni_{23}$ alloy shows a large discharge capacity(410 mA·h·g^{-1}), which is 1.3 times larger than that of AB_5 type alloys.

In this paper, the structure, microstructure, thermal stability and hydrogen storage properties of $La_{0.95}Mg_{2.05}Ni_9$ alloy prepared by mechanical alloying were investigated.

2 EXPERIMENTAL

2.1 Sample preparation

$La_{0.95}Mg_{2.05}Ni_9$ primary alloy was prepared as follows. A mixture of powders of lanthanum, magnesium and nickel was put into a stainless steel vial together with 80 stainless steel balls of 10 nm in diameter. Total amount of the powder mixture was 10.0 g. All above handlings were performed in a glove box under purified argon atmosphere. Then the mixture was mechanically alloyed for selected time(30, 50, 70 h) using a planetary ball mill apparatus(QM—1SP4) with rotating speed of 400 r/min.

The test electrode was fabricated from 0.25 g mechanically alloyed $La_{0.95}Mg_{2.05}Ni_9$ specimen, mixed with electrolyte copper powder in a mass ratio of 1∶2, and then fixed with Teflon(PTFE) solution onto a foam nickel holder. The test battery was prepared by wrapping the electrode with a Nylon nonwoven fabric separator. This anode was tightly sandwiched between two plates of the nickel oxide positive cathode. The assembly was put in a container, filled with 6 mol/L KOH electrolyte solution. In order to examine the tendency for discharge loss on the hydride anode, the construction of test battery was de-

① **Foundation item:** Project(50171024) supported by the National Natural Science Foundation of China; project(0135053) supported by the Natural Science Foundation of Guangxi Province, China

Received date: 2003－08－27; **Accepted date:** 2004－01－30

Correspondence: MENG Miao-wu; Tel: +86-773-5601434; E-mail: mmwmmw@mailbox.gxnu.edu.cn

signed for an anode capacity-limited system.

2.2 Sample characterization

The structural properties, microstructure and thermal stability of samples were examined by X-ray diffractometer(XRD, D8 Advance) with CuK_α radiation(λ= 0.154 1 nm), differential thermal analysis (DTA), scanning electron microscopy(SEM, JSM-5100LV), respectively. The DTA was carried out under a purified argon atmosphere under a heating condition of 10 $K \cdot min^{-1}$ up to 793 K. Mass of the sample was nearly 0.025 g.

The electrochemical hydrogen storage properties of the test battery were conducted at ambient temperature using a DC-5B automatic battery test apparatus with PC computer and charge/discharge controlling software. The sample cell was charged for 5 h at 100 $mA \cdot g^{-1}$, and then discharged at various currents to a 0.9 V cutoff voltage. After each charging or discharging, the circuit was opened for 10 min.

3 RESULTS AND DISCUSSION

3.1 Structural characteristics

The XRD patterns of the mechanically alloyed $La_{0.95}Mg_{2.05}Ni_9$ samples were depicted in Fig. 1.

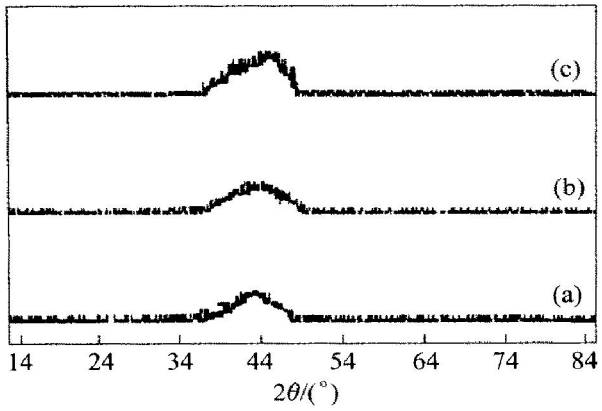

ig. 1 X-ray diffraction patterns of $La_{0.95}Mg_{2.05}Ni_9$ alloy prepared by mechanical alloying for selected time at 400 r/min
(a) —30 h; (b) —50 h; (c) —70 h

As can be seen from curve (a) in Fig. 1, the $La_{0.95}Mg_{2.05}Ni_9$ specimen synthesized by mechanical alloying for 30 h at the rotating of 400 r/min shows no sharp peak in its diffraction pattern and exhibits a broad diffuse peak at around 38 – 48° which indicates that the sample has an amorphous structure. By comparing curves(b) and (c) with (a) in Fig. 1, it is found that the amorphous phase structure cannot be changed with increasing the mechanical alloying time, but the maximum position of the halos shifts a little to higher angle.

3.2 Analysis of thermal stability

The thermal stability of amorphous specimens during heat treatment was examined by DTA, and the results were represented in Fig. 2.

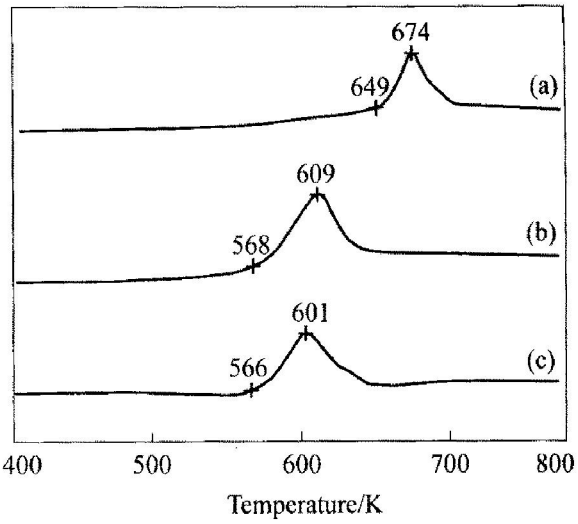

Fig. 2 DTA curves of $La_{0.95}Mg_{2.05}Ni_9$ alloy synthesized by mechanical alloying for selected time at 400 r/min
(a) —70 h; (b) —50 h; (c) —30 h

From curve (c) in Fig. 2, we observed only one exothermic reaction around 601 K in the DTA pattern of amorphous $La_{0.95}Mg_{2.05}Ni_9$ alloy prepared by mechanical alloying for 30 h at 400 r/min, corresponding to the crystallization temperature of the specimen. By comparing curves (b) and (a) with (c) in Fig. 2, we can see that shape of the DTA curves did not change with increasing mechanical alloying time, but the exothermic peak shifts to higher temperature, which implies that the thermal stability of the amorphous specimens are improved with increasing mechanical alloying time.

3.3 Activation behavior

The first activation curves of $La_{0.95}Mg_{2.05}Ni_9$ alloy electrodes were depicted in Fig. 3(At a charge current of 100 $mA \cdot g^{-1}$ and discharge current of 50 $mA \cdot g^{-1}$).

As can be seen from the charge curves in Fig. 3, there is slightly difference among the specimens synthesized by mechanical alloying for selected time at 400 r/min. On the other hand, there exists remarkably difference in the discharge curves among the samples. In the cases of discharge curves (c) and (b) in Fig. 3, a plateau of the discharge voltage was observed, and the plateau voltage of the electrode alloy synthesized by mechanical alloying for 30 h at 400 r/min was more positive than that of the other specimens, suggesting that good hydrogen absorb/desorb ability of $La_{0.95}Mg_{2.05}Ni_9$ alloy has been obtained by

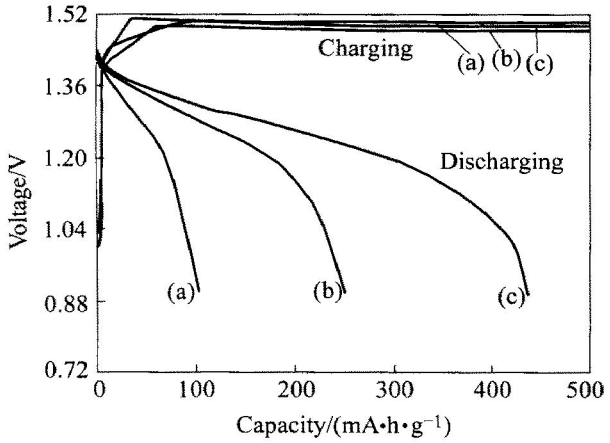

Fig. 3 Electrochemical activation curves of specimens synthesized by mechanical alloying for selected time at 400 r/min
(a) —70 h; (b) —50 h; (c) —30 h

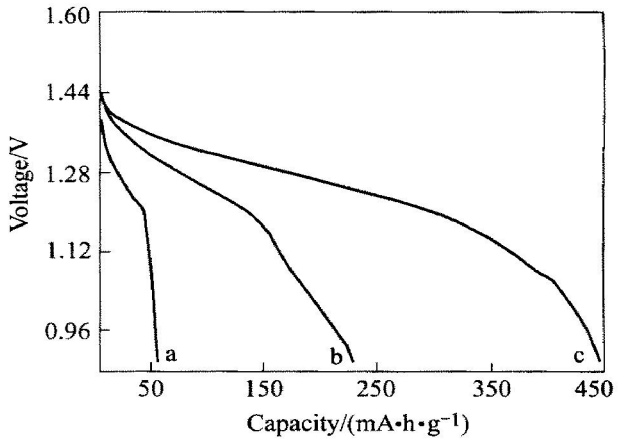

Fig. 4 Discharge curves of specimen using MA (400 r/min for 30 h) $La_{0.95}Mg_{2.05}Ni_9$ alloy at different discharge currents
(a) —400 mA·g^{-1}; (b) —200 mA·g^{-1}; (c) —20 mA·g^{-1}

mechanical alloying for appropriate time at 400 r/min probably due to the change of equilibrium pressure of hydrogen. On the other hand, the plateau voltage would decrease seriously with increasing mechanical alloying time as curves (b) and (a) shown in Fig. 3. Moreover, under this experimental condition, the maximum discharge capacity of specimen prepared by mechanical alloying for 30 h at 400 r/min is 430 mA·h·g^{-1} at a discharge current of 50 mA·g^{-1} at first electrochemical charge/discharge cycle.

3.4 Effects of discharge current on capacity

Fig. 4 showed the typical discharge curves of test battery at different discharge currents.

In Fig. 4, the discharge capacity of the test battery decreased with increasing discharge current. The discharge capacity obtained at a discharge current density of 200 mA·g^{-1} and 400 mA·g^{-1} were approximately 52% and 13%, respectively, of the values obtained at 20 mA·g^{-1}. The discharge capacity dependence on the discharge current density might be explained as follows. Increasing discharge current causes an increase in polarization of both the anode and the cathode of the test battery. This in turn results in a correspondingly reduced cell voltage when a high discharge rate is applied, leading to a smaller discharge capacity.

3.5 Cyclic stability

The change in discharge capacities of the amorphous $La_{0.95}Mg_{2.05}Ni_9$ alloy synthesized by mechanical alloying for 30 h at 400 r/imn with the number of cycles was shown in Fig. 5(At a charge current of 100 mA·g^{-1} and discharge current of 20 mA·g^{-1}).

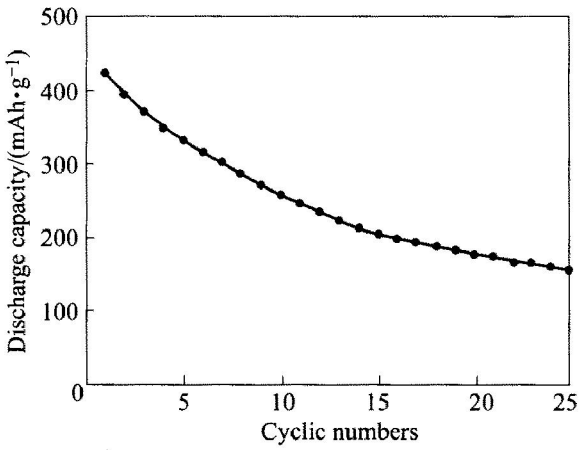

Fig. 5 Discharge capacities as a function of cyclic numbers for $La_{0.95}Mg_{2.05}Ni_9$ alloy prepared by MA (400 r/min for 30 h)

From Fig. 5, $La_{0.95}Mg_{2.05}Ni_9$ alloy synthesized by mechanical alloying for 30 h at 400 r/min reached its maximum electrochemical discharge capacity at the first charge/discharge cycle and possessed good activation characteristics, which should be attributed to its amorphous structure (as shown in Fig. 1). Nevertheless, the discharge capacity decreased seriously with increasing cyclic numbers before 15th cycles, and then the tendency of capacity degradation became smaller than that for the former cycles. Overall, the discharge capacity of the specimen was about 35% of the initial capacity after 25th cycles.

3.6 Mechanism of capacity degradation

In order to study the causes of discharge capacity loss of amorphous $La_{0.95}Mg_{2.05}Ni_9$ alloy electrodes during charge/discharge cycling, the XRD and SEM analysis for charged/discharged specimens were car-

ried out, and the results were depicted in Figs. 6 and 7.

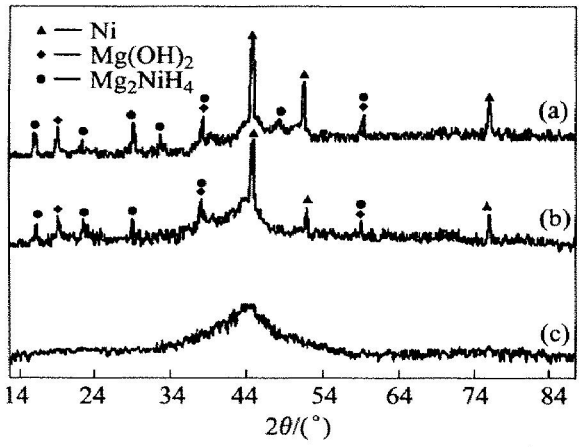

Fig. 6 X-ray diffraction patterns of MA $La_{0.95}Mg_{2.05}Ni_9$ specimens after different cycles(400 r/min for 30 h)
(a) —25th cycle; (b) —15th cycles; (c) —1st cycles

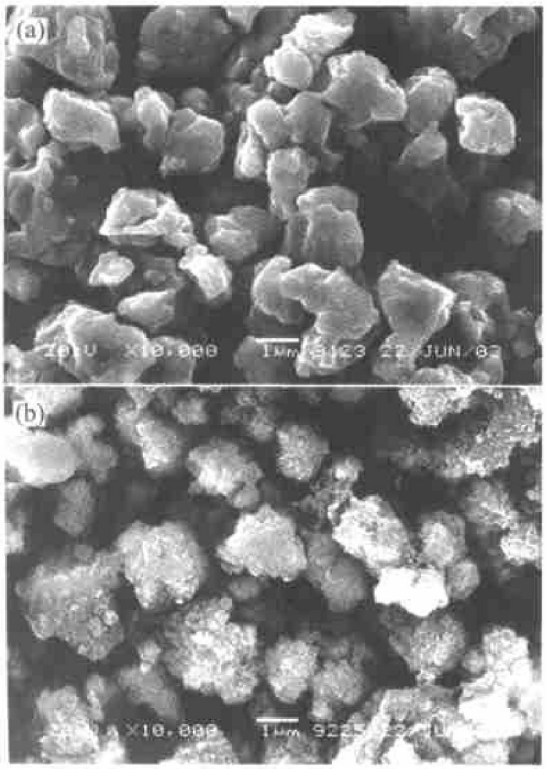

Fig. 7 SEM images of as-mechanically-alloyed and as-hydrided $La_{0.95}Mg_{2.05}Ni_9$ specimens
(a) —Mechanical alloying for 30 h at 400 r/min; (b) —After 25th cycling

As can be seen from curve (c) in Fig. 6, the amorphous structure of specimen did not change at the first electrochemical cycle, but the peaks of Ni, Mg_2NiH_4 and $Mg(OH)_2$ phases appeared clearly at the 15th charge/discharge cycles as curve (b) shown in Fig. 6.

By comparing curve (a) with (b) in Fig. 6, it is found that intensities of the crystalline phases strengthened gradually and the amorphous content in the alloy decreased during the cyclic tests, suggesting that partially amorphous phase decomposed to the crystalline Mg_2NiH_4 and Ni phases during electrochemical charge/discharge cycling.

Fig. 7 showed SEM images of the as-alloyed and as-hydrided specimens. By comparing (b) with (a) in Fig. 7, there was not major difference in shape (sphere or spheroid) and in size(0.7 – 4.0 μm) between the specimens synthesized by mechanical alloying for 30 h at 400 r/min and charging/discharging for 25th cycles in 6 mol/L KOH electrolyte, but the surface state of the particles was different. In the case of specimen for 25 electrochemical cycling, some small particles of Mg-$(OH)_2$ could be seen on particles surface. It is known that the magnesium alloys have poor corrosion resistance, especially when they are in contact with strongly corrosive media. The results shown in Fig. 6 suggested that the surface of the magnesium alloy is covered by $Mg(OH)_2$ during charge/discharge cycling. When the partial alloy is oxidized to $Mg(OH)_2$, the amount of hydrogen storage alloy is consequently reduced. As the oxidation forms on the surface of the electrode, both charge-transfer at the alloy/electrolyte interface and hydrogen diffusion either into or out from the bulk alloy when charging(or discharging) are inhibited, which leads to a lower discharge capacity.

Therefore, the reason of discharge capacity loss of amorphous $La_{0.95}Mg_{2.05}Ni_9$ electrodes was that the amorphous phase decomposed to crystalline Mg_2NiH_4 and Ni phases and Mg on the surface was oxidized to $Mg(OH)_2$ during the electrochemical charge/discharge cycles in 6 mol/L KOH electrolyte.

4 CONCLUSIONS

1) Amorphous $La_{0.95}Mg_{2.05}Ni_9$ alloy is prepared by mechanical alloying for 30 – 70 h at 400 r/min, and the thermal stabilities of the amorphous specimens are improved with increasing the mechanical alloying time.

2) The test battery using $La_{0.95}Mg_{2.05}Ni_9$ alloy synthesized by mechanical alloying at 400 r/min for 30 h shows good charge/discharge behavior(430 $mA \cdot h \cdot g^{-1}$) at room temperature, but the discharge capacity decreases seriously during the electrochemical charge/discharge cycle tests. The discharge capacity loss are attributed to two factors: one is partially amorphous phase decomposes to the crystalline Mg_2NiH_4 and Ni phases with increasing charge/discharge cyclic number. The other is the surface oxidation of the magnesium alloy in an alkaline aqueous solution forms $Mg(OH)_2$ phase, that in turn causes a reduction in capacity and inhibition hydrogen mass transfer.

REFERENCES

[1] Yuan H, Cao R, Wang L B, et al. Characteristics of a new Mg-Ni hydrogen storage system: $Mg_{2-x}Ni_{1-y}Ti_xMn_y$ alloys[J]. J Alloys Compounds, 2001, 322: 246-248.

[2] ZHANG Yao, LI Shou-quan, YING Tiao, et al. Effect of surface coating by ball milling on cycle stability of Mg-based hydrogen storage electrodes[J]. The Chinese Journal of Nonferrous Metals, 2001, 11(4): 582-586. (in Chinese)

[3] Chen J, Yan P, Bradhurst D H, et al. Mg_2Ni-based hydrogen storage alloys for metal hydride electrodes[J]. J Alloys Compounds, 1999, 293-295: 675-679.

[4] YU Zhen-xing, LIU Zu-yan, WANG Er-de. Influence of $CrCl_3$ on hydrogen storage properties of Mg-Ni systems [J]. The Chinese Journal of Nonferrous Metals, 2001, 11(6): 1032-1036. (in Chinese)

[5] Ikeda K, Orimo S, Zuttel A, et al. Cobalt- and copper-substitution effects on thermal stabilities and hydriding properties of amorphous MgNi[J]. J Alloys Compounds, 1998, 280: 279-283.

[6] WANG Zhong-min, ZENG Mei-qing, YANG Yong-qiang, et al. Effect of mechanical alloying on formation of Mg_2Ni[J]. The Chinese Journal of Nonferrous Metals, 2001, 11(2): 236-239. (in Chinese)

[7] Iwakura C, Iroshi H, Zhang S G, et al. A new electrode material for nickel-metal hydride batteries: MgNi-graphite composites prepared by ball-milling[J]. J Alloys Compounds, 1999, 293-295: 653-657.

[8] Berlouis L E A, Cabrera E, Hall-Barientosss E, et al. A thermal analysis investigation of the hydriding properties of nanocrystalline Mg-Ni based alloys prepared by high energy ball milling[J]. J Alloys Compounds, 2000, 30: 582-589.

[9] Terashita N, Takahashi M, Kobayashi K, et al. Synthesis and hydriding/dehydriding properties of amorphous $Mg_2Ni_{1.9}M_{0.1}$ alloys mechanically alloyed from $Mg_2Ni_{1.9}M_{0.1}$ (M= none, Ni, Ca, La, Y, Al, Si, Cu and Mn) and Ni powder[J]. J Alloys Compounds, 1999, 293-295: 541-545.

[10] Cui N, Luan B, Zhao H J, et al. Effects of yttrium additions on the electrode performance of magnesium-based hydrogen storage alloys[J]. J Alloys Compounds, 1997, 259: L5-L8.

[11] Kadir K, Noreús D, Yamashita I. Structural determination of $AMgNi_4$ (where A= Ca, La, Ce, Pr, Nd and Y) in the $AuBe_5$ type structure[J]. J Alloys Compounds, 2002, 345: 140-143.

[12] Liang G, Huot J, Baily S, et al. Hydrogen storage in mechanically milled Mg-$LaNi_5$ and MgH_2-$LaNi_5$ composite[J]. J Alloys Compounds, 2000, 297: 261-265.

[13] Gross K J, Spatz P, Zuttel A, et al. Mechanically milled Mg composites for hydrogen storage—the transition to a steady state composition[J]. J Alloys Compounds, 1996, 240: 206-209.

[14] Schmid J, Sommer F. Heat capacity of liquid La-Mg-Ni alloys[J]. J Alloys Compounds, 1998, 266: 216-223.

[15] Tanaka K, Kanda Y, Furuhashi M, et al. Improvement of hydrogen storage properties of melt-spun Mg-Ni-RE alloys by nanocrystalline[J]. J Alloys Compounds, 1999, 293-295: 521-525.

[16] Kohno T, Yoshida H, Kawashima F, et al. Hydrogen storage properties of new ternary system alloys: La_2MgNi_9, $La_5Mg_2Ni_{23}$, La_3MgNi_{14} [J]. J Alloys Compounds, 2000, 311: L5-L7.

(Edited by HUANG Jin-song)